



HAL
open science

Meso-Macro Optical Experimental Analysis of Woven Composite Reinforcement in Plane Shear during their Forming

Gilles Hivet, Jérôme Launay, Philippe Boisse

► **To cite this version:**

Gilles Hivet, Jérôme Launay, Philippe Boisse. Meso-Macro Optical Experimental Analysis of Woven Composite Reinforcement in Plane Shear during their Forming. *Finite International Journal of Forming Processes*, 2005, 8, pp.157-167. hal-00081073

HAL Id: hal-00081073

<https://hal.science/hal-00081073>

Submitted on 2 May 2023

HAL is a multi-disciplinary open access archive for the deposit and dissemination of scientific research documents, whether they are published or not. The documents may come from teaching and research institutions in France or abroad, or from public or private research centers.

L'archive ouverte pluridisciplinaire **HAL**, est destinée au dépôt et à la diffusion de documents scientifiques de niveau recherche, publiés ou non, émanant des établissements d'enseignement et de recherche français ou étrangers, des laboratoires publics ou privés.



Distributed under a Creative Commons Attribution - NonCommercial 4.0 International License

Meso-Macro Optical Experimental Analysis of Woven Composite Reinforcement in Plane Shear during their Forming

Gilles Hivet* — Jean Launay* — Philippe Boisse*,**

* *Laboratoire de Mécanique des Systèmes et des Procédés
LMSP, UMR CNRS ENSAM-Polytech'Orléans
8 rue Léonard de Vinci, F-45072 Orléans cedex*

** *Laboratoire de Mécanique des Contacts et des Solides
LaMCoS, UMR CNRS 5514, INSA de Lyon, Bâtiment Jean d'Alembert
18-20, rue des Sciences, F-69621 Villeurbanne cedex
{gilles.hivet, jean.launay}@univ-orleans.fr
philippe.boisse@insa-lyon.fr*

ABSTRACT. The in-plane shear behaviour is important in woven composite reinforcement forming processes. It is the largest strain mode when forming a double curved surface. The shear locking angle is a limit to the feasibility of a given shape. This paper presents an experimental study of this in-plane shear mechanical behaviour using a picture frame device and strain optical analyses. These measurements are based on a correlation method and are performed both at macro scale (scale of the picture frame) and at meso-scale (scale of the yarn). The first measures permit to check the uniformity of the strain field and to choose between different technologies and especially the clamping devices. The local analysis shows that the strains within the yarn are very different to the global strain. The yarn is mainly submitted to rigid rotation before the shear locking angle and crushed after. Shear in plane curves are especially given in this study for fabric chosen in the ESAFORM benchmark on composite forming.

KEYWORDS: Fibre Fabric Forming, in Plane Shear, Picture Frame, Meso-Macro Analysis, Optical Measures, Image Correlation.

1. Introduction

The ability for a fabric to be formed mainly depends on its in-plane shear behaviour. Many shear tests have been developed for metallic materials and shear mechanisms are fairly well known. Shear tests on composite materials are much more difficult to perform because those materials are heterogeneous and their structure is much more complex. The picture frame test is supposed to lead to a pure in-plane shear loading. Many studies have already been performed in order to identify the shear behaviour for composite materials (Long, 2002; Lussier *et al.*, 2002; Mohammed *et al.*, 2000; Kawabatta *et al.*, 1973). Curves giving the shear angle as a function of the force applied on the deformable frame may be found in the literature. Some other information may be necessary to understand much better what happens during the shear deformation of fabrics. It seems sensible to assess that the kinematics of the frame is well transmitted to the sample. The local repartition of the strains is also very interesting. The use of optical methods makes it possible to obtain displacement fields. Changing the lens allows to make multi-scale measurements (Dumont *et al.*, 2003), thus the measure is done directly on the sample, so it is possible to compare the prescribed displacements really imposed to the sample with the one that was supposed to be.

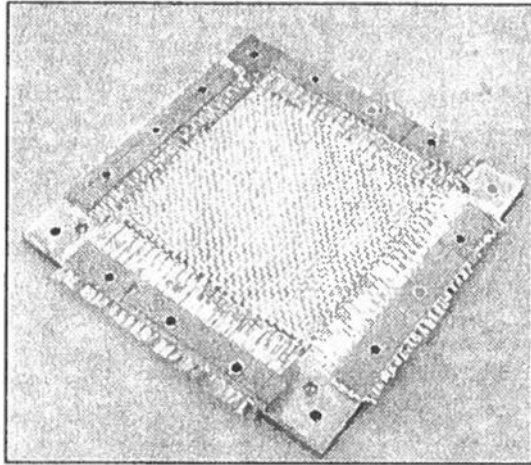
2. Experimental device

To perform the picture frame test, a deformable frame is put on a traction device that prescribes the displacement of the frame's upper pin (Figure 1b). The traction compression device gives the global displacement and the prescribed load. The displacement rate can be controlled from 0 to 1 m/min. Two cameras with two different lenses are fixed on the device. The first enables to see the full displacement field on the sample. With the second, the field is reduced to 12.4*9.6 mm². Consequently, simultaneous measures at the mesoscopic scale (yarn's scale) and at the macroscopic scale can be performed. The device gives three measures of displacement: the one given by the picture frame, and the macroscopic and mesoscopic ones, given by cameras. To obtain the strain field, an image correlation method is used (Raffel *et al.*, 1998; Dumont *et al.*, 2003). The comparison between all these values is very helpful to understand the behaviour of fabrics during the test.

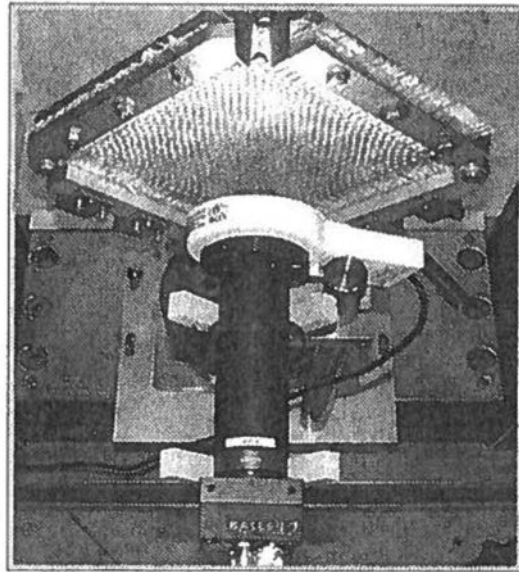
3. Analysis of picture frame results

Shear angle curves of many materials have already been given in the literature. Different steps have been identified during deformation of the fabric. Meso optical measures can be used to analyse these different steps. The displacement field on a yarn during the picture frame test precisely points out the behaviour of an individual yarn. But the most interesting point comes from the comparison between meso and

macro results, because it allows us to understand what happens during the test and localise the events on the global shear curves. It links local phenomena on an individual yarn to the global shear behaviour of the sample.



a) Fabric sample with plates

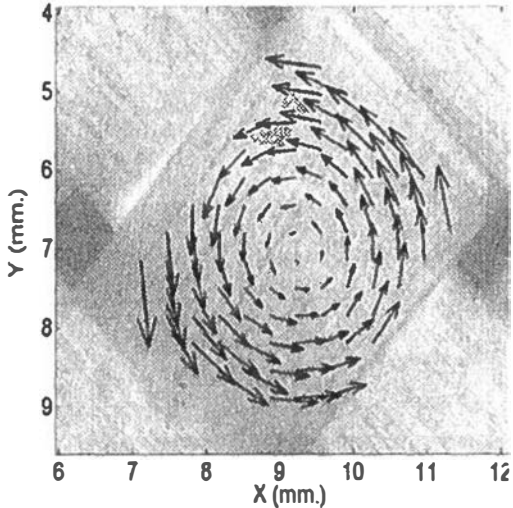


b) Experimental device

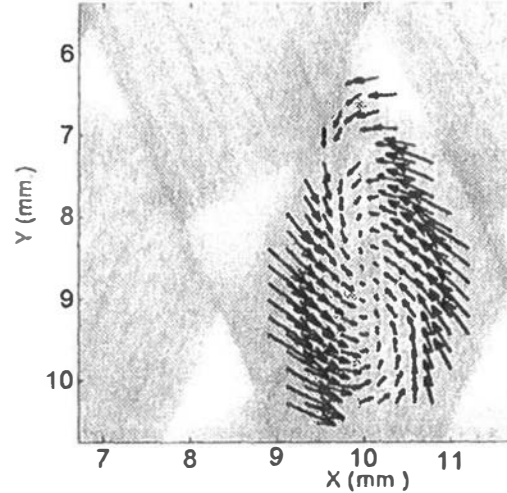
Figure 1. *Experimental device*

Three parts may be identified on the shear curve (Figure 4) as it is usually admitted in the literature. The first one (part 1, Figure 4) corresponds to the weak shear rigidity of the fabric. The displacement field obtained (after subtracting the average displacement) on a yarn is characteristic of a rigid body rotation (Figure 2a). This proves that no shear of the yarn itself happens during the first part of the test. The yarn rotate but are not sheared themselves (Wang *et al.*, 1999). After this first part the curve makes a bend, shear stiffness begins to increase (part 2, Figure 4). A modification of the displacement field can be noticed on Figure 2b. During the first step, spacing between the yarns reduces and then contact between neighboring yarns occurs. But when observing different zones of the same sample, the contact does not appear simultaneously everywhere. The dispersions in yarns geometry of the same sample imply that a spacing closure is a progressive phenomenon. When contact occurs, the displacement field is the composition between rotation and transverse crushing. When the shear angle increases, the reorganization of fibers leads to a significant transverse compression of yarns, as can be seen Figure 2d (around 20% here). The round part of the curve is therefore due to the progressive closure of the spaces and the progressive increase of transverse stiffness. In the third part of the curve (part 3, Figure 4) the yarn is strongly crushed (Figure 2c). The apparition of wrinkles can be identified by the use of 3D stereoscopic measurement (Dumont *et al.*, 2003). Finally, Meso macro optical measurements allow us to point out clearly mechanisms involved during the picture frame test. Our goal is to obtain valuable

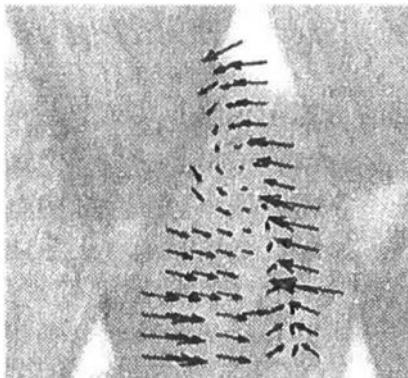
numerical results concerning the shear behaviour of fabrics that might be implemented in finite element codes (Daniel *et al.*, 2003). We used similar techniques to investigate to what extent the picture frame test is representative of the real pure shear behaviour of fabrics.



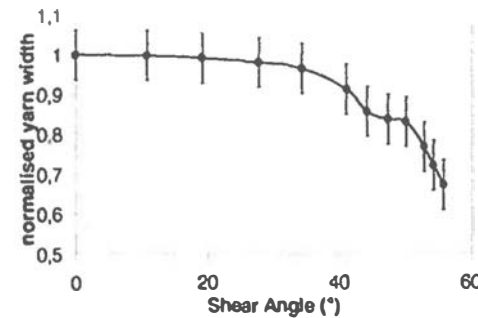
a) Displacement field in the first part of the shear curve



b) Displacement field in the second part of the shear curve



c) Displacement field in the third part of the shear curve



d) Evolution of the normalized yarn width

Figure 2. Fabric evolution during the picture frame test

4. Loading of the specimen

4.1. Homogeneity of the shear angle

If we accept that the first part of the curve is pure rotation of yarns, each yarn should be articulated on the picture frame (Mohammed *et al.*, 2000; McGuinness *et al.*, 1998). The practical achievement of such hinged boundary seems to provide better limit conditions but it is restricted to large yarns and low yarn density fabrics.

Furthermore, it is very difficult to realize. Positioning the sample is difficult and time consuming. Two other techniques are commonly used: clamping the fabric directly on the frame (Long, 2002), or clamping the sample through plates (Dumont *et al.*, 2003). Two types of plates can be used. If plates are made of prepreg, sample is heated to obtain the polymerization of the plates. In the other case, plates and sample are glued using silicon glue. In both cases, yarns are completely attached to the plates. No sliding is possible between frame and sample.

The results concerning the homogeneity of the shear strains are presented in Figure 3. It appears that the presence of plates significantly enhances the homogeneity of the field; the heterogeneity is reduced to less than 10% in the case presented here.

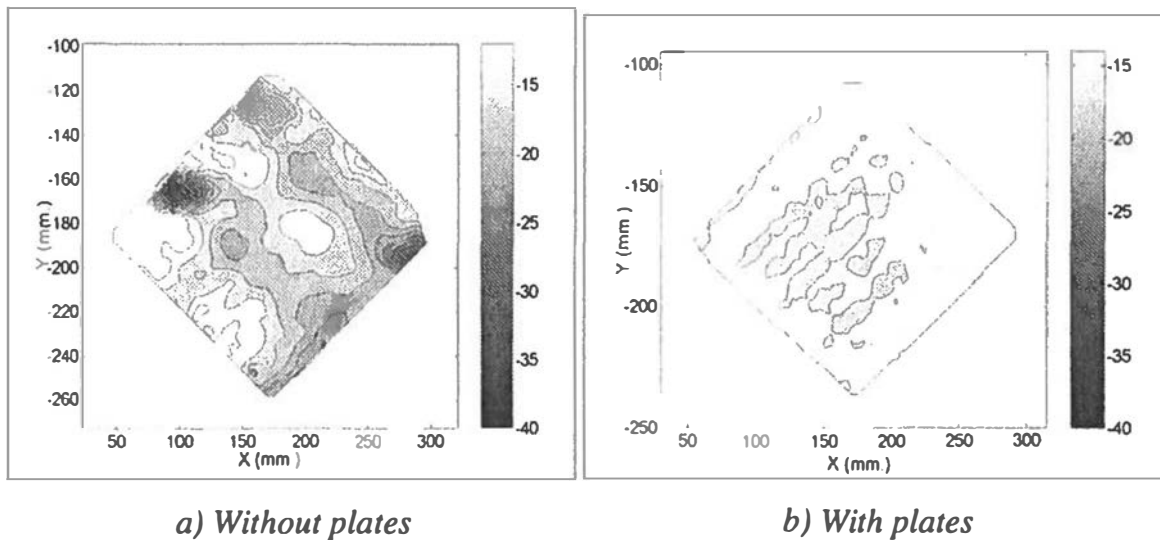


Figure 3. Homogeneity of the log deformation of the sample 4.2. Influence of plate type

The main difference between the plates concerns the modification of the fabric behaviour. The more rigid the plate is, the more the behaviour of the fabric is affected. Using some aramid prepreps leads for example to the premature failure of yarns and to huge increase in shear rigidity. The best plate appeared to be the aluminium one with a silicone glue that ensures a good homogeneity of the field with the slightest interaction on the fabric behaviour. This type of plates will always be used for further tests.

4.2. Bending of yarns close to the frame bars

The comparison between the angle of the picture frame and the one measured on the fabric is presented for a glass fabric on Figure 4. The difference between the two

curves is noticeable especially at the end of the test. Observing the edges of the sample points out the limit conditions problems we have discussed before; yarns are not hinged, so they have to bend to be able to rotate (Figure 5). The yarn then has an S form (Dumont *et al.*, 2003; Mohammed *et al.*, 2000). Two conclusions may be made; the main shear mechanism is yarn rotation, because it occurs whereas yarns are not hinged so that they are not supposed to rotate. The second conclusion is that the shear angle seen on the sample is different from the one imposed by the picture frame test. This difference may reach 5 to 10 degrees at the end of the test. Performing picture frame tests on fabrics is very difficult and poses many problems. Many precautions must be taken to obtain a homogeneous shear solicitation on the sample. Optical measures allowed us to underline these problems especially the issue with limit conditions on the sample. They also permit to validate a given test by measuring a correctly homogeneous strain field. Improving boundary conditions is an important point to obtain a more representative test.

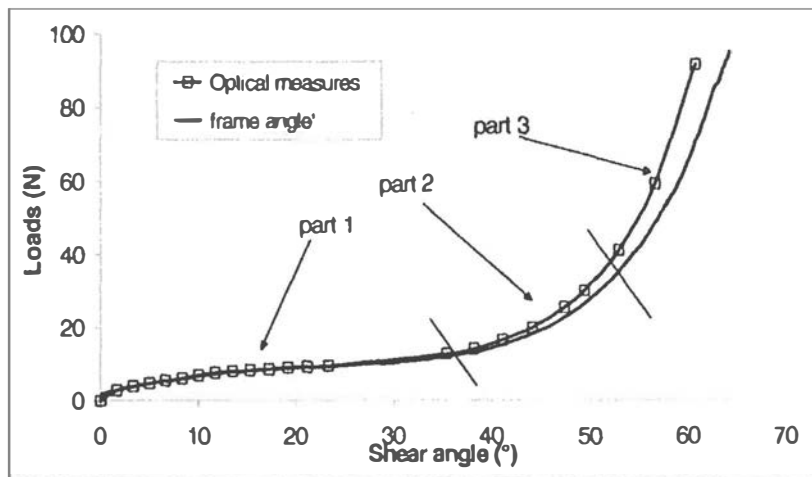


Figure 4. Comparison between frame angle and real shear angle between yarns

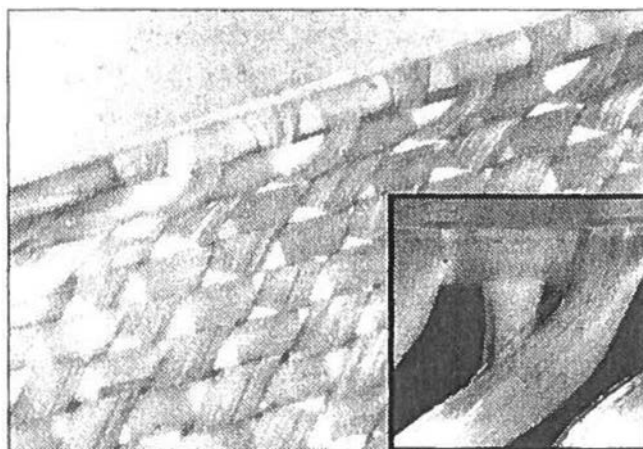


Figure 5. Bending of yarns close to frame bars

5. Picture frame tests on benchmark fabrics

The presented results are obtained on the three fabrics chosen in the benchmark on woven composite reinforcements coordinated by J. Cao (Cao *et al.*, 2004) a twintex® plain weave, two different twintex® twill weaves (a Twintex® fabric is made using co-mingled glass/polypropylene yarns, Figure 6). Even though the three fabrics have a very different structure, curves found for benchmark fabrics have a similar shape that is representative of the one traditionally found for fabric shear curves. For all the fabrics, when the same sample is re-tested, a relaxation of the shear stiffness occurs after the first or first two tests. After the fourth test, stabilization can be seen (Figure 7). This can be attributed to the initial positioning of yarns and to little modifications in yarn's structure. This phenomenon has already been observed for other fabrics in the literature (Lussier *et al.*, 2002). The loading rate seems to influence the dispersion and precision of the measures. Concerning the measured shear stiffness, no influence has been noticed (Figure 8) which is consistent with some other results (Mohammed *et al.*, 2000; McGuinness *et al.*, 1998). More tests are currently in progress to confirm this trend.

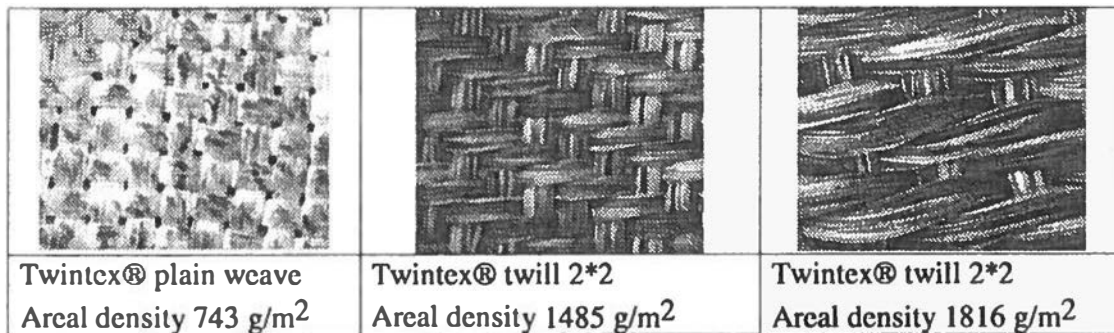


Figure 6. Benchmark fabrics

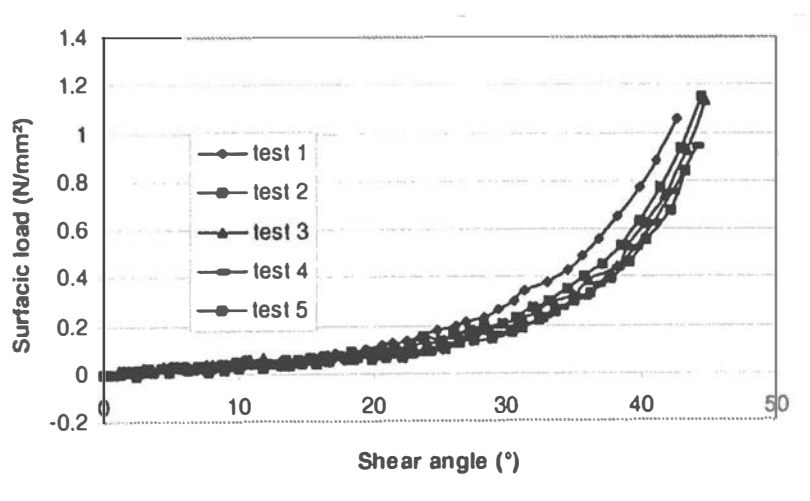
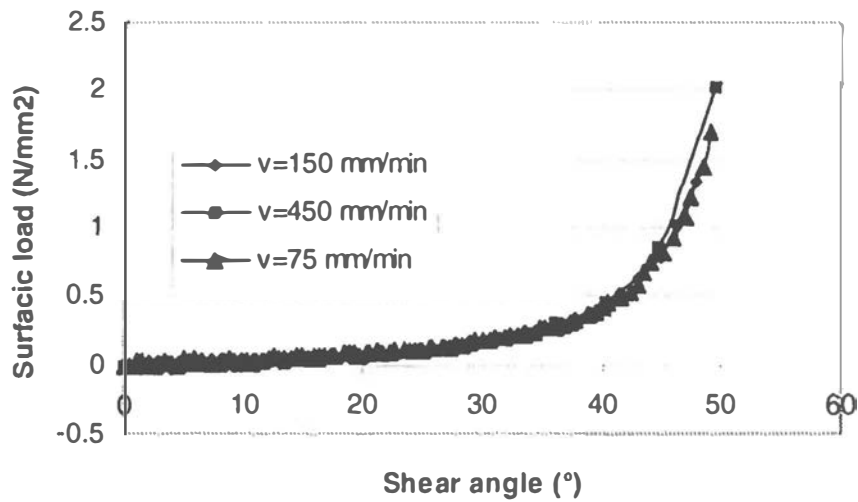
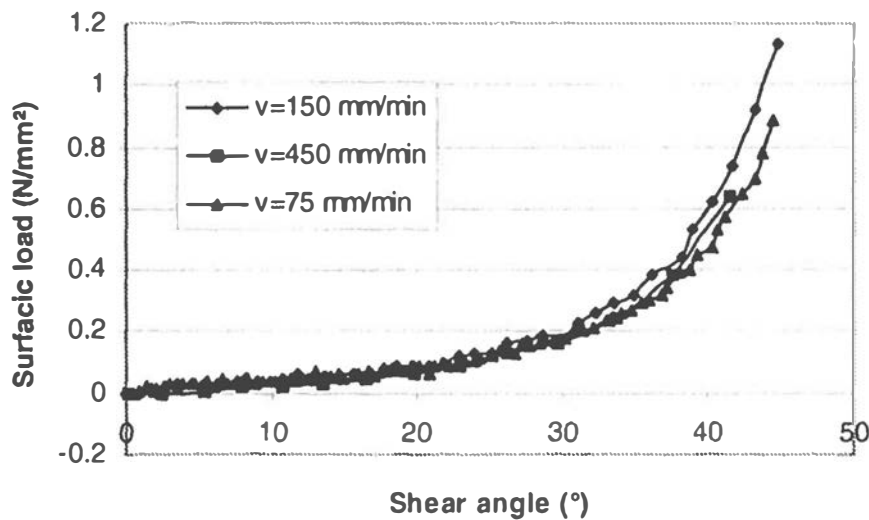


Figure 7. Repeatability of the picture frame test, on the same sample, for the benchmark fabrics. Twintex® twill 2*2 Areal density 1485 g/m²



a) Twintex® plain weave Areal density 743 g/m²



b) Twintex® twill 2*2 Areal density 1485 g/m²

Figure 8. Evolution of the shear curve as a function of deformation rate

6. Use of in-plane shear behaviour in forming simulation

The yarns of the fabric considered in this paper (those classically used as textile composite reinforcements) are made of thousands of small fibres (glass, carbon or aramid). Warp and weft yarns are woven following classical weavings (plain, satin, twill) (Figure 9).

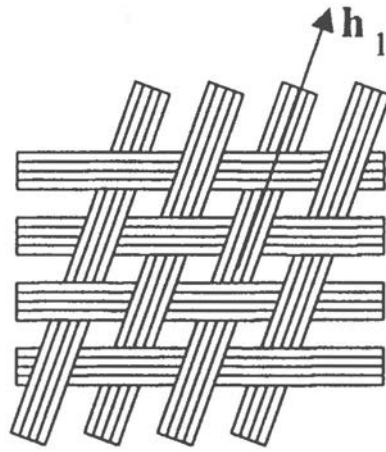


Figure 9. Woven yarns made of juxtaposed small fibres

This constitution leads to a very specific mechanical behaviour of the fabric. Most of the rigidities are small or very small in comparison to tensile stiffness in the yarn directions. An efficient model of the mechanical behaviour of the fabric will only account for the significant mechanical quantities. Nevertheless the model will have to describe the specificities of textile reinforcement mechanical behaviour, especially:

- the tensile behaviour of the yarns;
- the very different in plane shear behaviour before and after the locking angle.

The diameter of the glass, carbon or aramid fibres is very small (some μm) regarding to their length. Consequently they can only be submitted to tension in the direction \mathbf{h}_1 of the yarn. The Cauchy stress tensor in a yarn in tension is:

$$\boldsymbol{\sigma} = \sigma^{11} \mathbf{h}_1 \otimes \mathbf{h}_1 \quad [1]$$

The tension in the yarn is often easier to measure (A is the section of the yarn):

$$\mathbf{T}^{11} = \int_A \sigma^{11} dS \quad \mathbf{T} = T^{11} \mathbf{h}_1 \otimes \mathbf{h}_1 \quad [2]$$

The tensile mechanical behaviour of the fabric is completed by adding a shear rigidity to every yarn crossover (Boisse, 2005). The action between the warp and weft yarns can be modeled by a torque applied at the yarn intersections. The value of this shear torque for a shear angle is experimentally given by the picture frame test. To find the value of this resistant torque C , it is assumed that the fibres remain straight during the test. Consequently, all the angles (between warp and weft) and all the torques at the intersections are equal over the frame. The dissipated power is assumed to be small and consequently:

$$\mathbf{F} \cdot \mathbf{V}_c = N_c N_t C(\gamma) \quad [3]$$

\mathbf{F} is the load on the tensile machine, \mathbf{V}_c is the speed of the mobile part of the machine, N_c and N_t are the number of woven unit cells in warp and weft directions. The elementary torque according to the shear angle is given by:

$$C(\gamma) = \frac{a}{N_c N_t} \frac{\sqrt{2}}{2} \left(\cos \frac{\gamma}{2} - \sin \frac{\gamma}{2} \right) F(u(\gamma)) \quad [4]$$

$u(\gamma)$ is the displacement of the tensile machine corresponding to the angle γ . Consequently the knowledge of $F(\gamma)$ as given in Figure 4 gives $C(\gamma)$.

Taking only the tensile and in-plane shear strain energy into account, the global equation of the virtual work principle in dynamics can be written:

$$\sum_{p=1}^{\text{yarns}} \int_{p_1}^p \epsilon_{11}(\eta) T^{11} d\eta + \sum_{q=1}^{\text{crossovers}} C^q(\gamma(\eta)) - T_{ext}(\eta) = \int_{\Omega} \rho \ddot{u} \cdot \eta \, dV \quad [5]$$

$\forall \eta / \eta = 0$ on the boundary of the fabric with prescribed displacements.

A finite element approach can be introduced from this simplified dynamic equation (Boisse, 2005). The mechanical behaviour properties asked to perform the computation are the tensile behaviour of the yarn $T^{11}(\epsilon_{11})$ and the in plane shear behaviour $C(g)$. This last curve is given by the result of the picture frame $F(\gamma)$ by Equation [4].

It has been shown in (Boisse, 2005) that the in-plane shear behaviour is mainly important in wrinkle appearance in forming processes.

7. Conclusions

The in-plane shear behaviour of a fabric is important especially to describe wrinkles in forming processes (Prodomou *et al.*, 1997) and consequently to define the feasibility of a given manufacturing process. It has been shown in the present study that an optical strain field measurement can help to achieve a correctly homogenous strain field in a picture frame test and that the clamping technology of the specimen is very important for this homogeneity. The best results have been obtained using aluminum plate in the present work. The mesoscopic scale analysis has shown that before the shear locking angle the yarn has a rigid body rotation. After this locking angle the yarns are transversely crushed and the global in-plane rigidity is much increased. Performing picture frame tests on the fabrics of the benchmark has confirmed a relaxation of the stiffness during the two or three tests (depending on the tested fabric). No significant influence of the strain rate has been

found (Figure 8) in the tested range of speed. However it appears that the picture frame is delicate and other tests such as the bias tests that were previously considered as less accurate are currently tested at the LMSP.

8. References

- Boisse P., Zouari B., Gasser A., "A mesoscopic approach for the simulation of woven fibre composite forming", *Composite Science and Technology*, 65, 2005, p. 429-436.
- Cao J. *et al.*, "A Cooperative Benchmark Effort on Testing of Woven Composites", *Proceedings of the 7th ESAFORM Conference on Material Forming*, Trondheim, Norway, April 28-30, 2004, p 305-308.
- Daniel J.L., Soulat D., Dumont F., Zouari B., Boisse P., Long A.C., "Forming simulation of very unbalanced woven composite reinforcements", *International Journal of Forming Processes*, Vol. 6, No. 3-4, 2003.
- Dumont F., Hivet G., Rotinat R., Launay J., Boisse P., Vacher P., "Field measurements for shear tests on woven reinforcements", *Mécanique et Industrie*, No. 4, 2003, p. 627-635.
- Kawabata S., Niwa M., Kawai H., "The finite-deformation theory of plain-weave fabrics. Part III: the shear-deformation theory", *Journal of textile institute*, 1973.
- Long A. C., "Characterisation and modelling of fabric deformation during forming of textile composites", *International Journal of Forming Processes*, 4-3-4, 2002, p. 285-301.
- Lussier D. S, Chen J, "Material characterization of woven fabrics for thermoforming of composites", *Journal of Thermoplastic Composite Materials*, 15-6, 2002, p. 497-509.
- McGuinness G. B., O. Bradaigh C. M., "Characterisation of thermoplastic composite melts in rhombus-shear: the picture-frame experiment", *Composites Part A: Applied Science and Manufacturing*, 29-1-2, 1998, p. 115-132.
- Mohammed U., Lekakou C., Dong L., Bader M., "Shear deformation and micromechanics of woven fabrics", *Composites Part A*, 31-5, 2000, p. 299-308.63, 62-85.
- Prodromou A.G. and Chen J., "On the relationship between shear angle and wrinkling of textile composite preforms", *Composites Part A: Applied Science and Manufacturing*, 1997, 28, 5, p. 491-503.
- Raffel M., Willert C., Kompenhaus J., "Particule Image Velocimetry. A practical guide", *Experimental Fluid Mechanics*, 1, Berlin, Springer, 1998.
- Wang J., Paton R., Page J. R., "The draping of woven fabric and prepregs for production of polymer composite components", *Composites Part A*, 30-6, 1999, p. 757-765.